International Journal of Modern Physics: Conference Series


# Determination of $E$ and $G$ observables in $\eta$ photoproduction on the CLAS Frozen Spin Target (FROST)

Igor Senderovich,* B. T. Morrison, M. Dugger, B. Ritchie, R. Tucker for the CLAS Collaboration
*Arizona State University*
*P.O. Box 871504, Tempe, AZ 85287-1504, U.S.A.*
*Igor.Senderovich@asu.edu*

Received Day Month Year
Revised Day Month Year

Polarization observables are vital for disentangling overlapping resonances in the baryon spectrum. Extensive data have been collected at Jefferson Lab in Hall B with circularly and linearly polarized tagged photon beam incident on longitudinally polarized protons provided by the Frozen Spin Target (FROST). The focus of the described work is on $\eta$ photoproduction, which acts as an "isospin filter", isolating the $N^*(I=1/2)$ resonances. Preliminary results for the double-polarization observables $E$ and $G$ are presented. There are currently no data on these in the world database for $\eta$ photoproduction.

*Keywords*: helicity observables; photoproduction; polarized target

## 1. Introduction

Since the natural width of nucleon resonances (typically 100–300 MeV) is generally much larger than the spacing of those excited states, differential cross sections measurements alone are not sufficient to disambiguate the details of those excitations. Instead, the differential cross section must be supplemented by measurements of polarization observables, the behaviors of which give information on the underlying photoproduction amplitudes for a given resonance. Preliminary results for two such observables measured in $\eta$ photoproduction are presented here. The first is the helicity observable $E$, determined from an experiment with a circularly-polarized ($C$) photon beam and longitudinally ($z$) polarized protons, which results in a modulation of the differential cross section ($d\sigma/d\Omega$) such that:

$$\frac{d\sigma}{d\Omega} = \frac{d\sigma}{d\Omega}_0 \left(1 - P_z^T P_C^\gamma E\right) \tag{1}$$

The second is the double polarization observable $G$, determined with a linearly-polarized ($L$) photon beam and longitudinally polarized target:

$$\frac{d\sigma}{d\Omega} = \frac{d\sigma}{d\Omega}_0 \left(1 - P_L^\gamma \Sigma \cos 2\phi + P_L^\gamma P_z^T G \sin 2\phi\right) \tag{2}$$

*Work at Arizona State University is supported by the U. S. National Science Foundation.

where $P$ denotes the degrees of beam ($\gamma$) or target ($T$) polarization. Note that the beam asymmetry $\Sigma$ in the above expression must be determined simultaneously, or canceled in some manner, to determine $G$. The significance of using $\eta$ compared to $\pi^0$, lies in *isospin filtering*. Having total isospin of 0, detection of the $\eta$ restricts the possible isospin of the baryon excitation to the $N^*(I=1/2)$ family. This work is part of a larger program to achieve a complete experiment, beginning with the unpolarized cross section [1,2].

## 2. The Experiment

Polarized photon beams were prepared via bremsstrahlung of electrons from Jefferson Lab's CEBAF accelerator. Circular and linear polarization is achieved in the usual manner: polarization transfer from electrons and use of diamond crystal radiators, respectively. Free protons are polarized in butanol via dynamic nuclear polarization at 30 mK by the FROzen Spin Target (FROST) system, which achieves a polarization fraction of $\sim$85% [3].

The final state particles were detected by the CEBAF Large Acceptance Spectrometer (CLAS). CLAS is primarily a charged particle detector, installed in a toroidal magnetic field. Principal components for this study included drift chambers for tracking, and a scintillator-based time-of-flight system for particle identification. With this detector, the primarily neutral final states of the $\eta$ are mainly reconstructed via the missing mass technique.

To aid partial-wave analyses of the proton resonance spectrum, the $\eta$ photoproduction data was analyzed in 50 MeV center-of-mass energy ($W$) bins and 0.2-wide center-of-mass production polar angle ($\cos\theta_{\rm cm}$) bins.

## 3. *E* Observable

The polarization observable $E$ can be expressed as an asymmetry of counts from the two beam helicities:

$$E = -\frac{1}{P_z^T P_C^\gamma}\left(\frac{N_+ - N_-}{N_+ + N_-}\right) \tag{3}$$

Note that the yields $N$ refer only to exclusive $\eta$ production counts, whereas many other events are detected in the same mass region. This background is largely unpolarized and therefore vanishes in the numerator of the above equation. The denominator, however, requires explicit correction. Figure 1 shows the missing mass spectra for a sample analysis bin. A simultaneous fit is performed to the missing mass spectra of both helicities to determine the background contribution. A helicity difference is shown on the left plot, demonstrating that helicity asymmetry is present primarily in the $\eta$ region. However, slight overall offsets are observed, likely related to some remaining polarized background such as $\pi^+\pi^-$. These offsets are corrected by fitting the sidebands and calculating the yield under the peak accordingly. Figure 2 shows preliminary results for the $E$ observable starting at the $\eta$ threshold, where the value of $E$ is expected and is confirmed to be close to one.

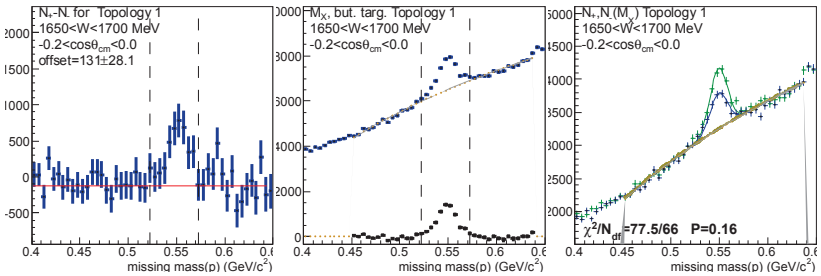


Fig. 1. Plots illustrating analysis of a kinematic bin to determine $E$. Fit of the background to the two helicities' missing mass spectra is shown on the right; background subtraction and net $\eta$ yield is shown in the middle. Helicity difference is shown in the left plot, where a fit to the side bands is performed to determine any overall asymmetry offset.

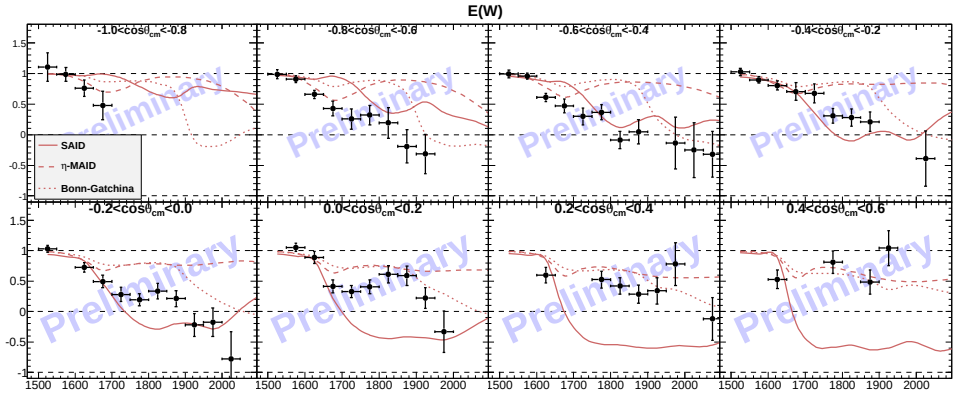


Fig. 2. Preliminary values of the helicity observable $E$ as a function of center of mass energy at various polar angles. Phenomenological fits prior to this data are identified in the legend.

## 4. *G* Observable

For the analysis of the $G$ observable, the data was binned somewhat differently: $W$ bins were overlapped to verify polarization between different photon beam coherent edge settings. The data was further binned in the azimuthal angle in order to extract $G$ from fits to the angular distribution. It is important to isolate the $G$ term because the overall asymmetry is dominated by the $\Sigma$ term. This is accomplished by a linear combination of $\phi$-dependent yields from different beam/target configurations, such as the following:

$$G\sin 2\phi = \frac{(P_\perp^+ + P_\parallel^-)(\tilde{N}_\parallel^+ P_\perp^- + \tilde{N}_\perp^- P_\parallel^+) - (P_\perp^- + P_\parallel^+)(\tilde{N}_\parallel^- P_\perp^+ + \tilde{N}_\perp^+ P_\parallel^-)}{P_\perp^- P_\parallel^+ (P_\perp^+ + P_\parallel^-)(|P_\perp^{z+}| + |P_\perp^{z-}|) + P_\perp^+ P_\parallel^- (P_\perp^- + P_\parallel^+)(|P_\perp^{z-}| + |P_\perp^{z+}|)} \quad (4)$$

To arrive at the normalized yields $\tilde{N}_i$, the following steps are made: a background fit to the missing mass spectrum is performed to determine the dilution of $\eta$ events in the overall event count. Variation of detector acceptance in $\phi$ is taken into account by dividing yields from data on amorphous targets, while the overall flux normalization

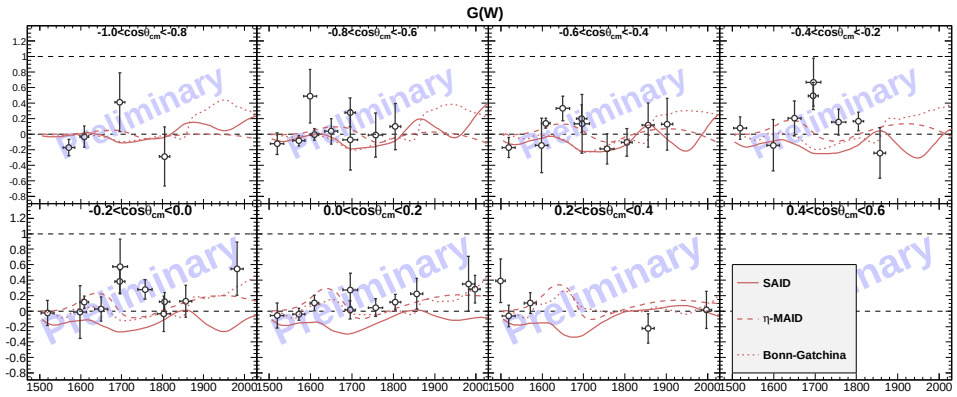


Fig. 3. Preliminary values of the $G$ observable as a function center of mass energy at different polar angles. The principal phenomenological fits prior to this data are given.

between the different beam/target settings is determined by fitting each $N_i(\phi)$ to the model $A(\phi) = N_0(1 + a\cos 2\phi + b\sin 2\phi)$. Thus, an individual configuration's normalized yield is defined as $\tilde{N}_i(\phi) \equiv N_i(\phi)\left[fN_0N_{\mathrm{AMO}}(\phi)\right]^{-1}$. The super-scripted signs label the longitudinal target polarization direction, while $\parallel$ / $\perp$ refer to the radiator crystal orientation with respect to the facility floor. Redundant labels on polarization fractions have been dropped for brevity. Beam and target configurations label all quantities to track their systematic variations across the run period.

The scarce statistics available to this analysis, and the expected values of $G$ close to zero make determinations difficult. Figure 3 shows the preliminary results for $G$, which are consistent with zero within the error bars, except for a distinct structure around 1700 MeV.

## 5. Conclusion

As no data on $E$ and $G$ from $\eta$ photoproduction have been published at this time, the results presented here will provide important constraints for understanding the proton spectrum. The values from phenomenological fits ([4, 5, 6]) not yet constrained by this data (shown on the same plots as the results) demonstrate the need for this experimental input.

## References

1. M. Dugger *et al.* [CLAS Collaboration], Phys. Rev. Lett. **89**, 222002 (2002) [Erratum-ibid. **89**, 249904 (2002)].
2. M. Williams *et al.* [CLAS Collaboration], Phys. Rev. C **80**, 045213 (2009)
3. E. Pasyuk [CLAS Collaboration], Chin. Phys. C **33** (2009) 1205
4. E. F. McNicoll *et al.* [Crystal Ball at MAMI Collaboration], Phys. Rev. C **82**, 035208 (2010) [Erratum-ibid. C **84**, 029901 (2011)] [arXiv:1007.0777 [nucl-ex]].
5. W.-T. Chiang, S.-N. Yang, L. Tiator, D. Drechsel, Nucl. Phys. A 700 (2002)
6. A. V. Anisovich, R. Beck, E. Klempt, V. A. Nikonov, A. V. Sarantsev and U. Thoma, Eur. Phys. J. A **48**, 15 (2012)